# Self-Stratification of Tropical Cyclone Outflow. Part I: Implications for Storm Structure

Kerry Emanuel

Program in Atmospheres, Oceans, and Climate

Massachusetts Institute of Technology

Cambridge, MA

Richard Rotunno

National Center for Atmospheric Research[1]

Boulder, CO

Abstract

Extant theoretical work on the steady state structure and intensity of idealized axisymmetric tropical cyclones relies on the assumption that isentropic surfaces in the storm outflow match those of the unperturbed environment at large distances from the storm's core. These isentropic surfaces generally lie just above the tropopause, where the vertical temperature structure is approximately isothermal, so it has been assumed that the absolute temperature of the outflow is nearly constant. Here we show that this assumption is not justified, at least when applied to storms simulated by a convection-resolving axisymmetric numerical model, in which much of the outflow occurs below the ambient tropopause and develops its own stratification, unrelated to that of the unperturbed environment. We here propose that this stratification is set in the storm's core by the requirement that the Richardson Number remain near its critical value for the onset of small-scale turbulence. We test this ansatz by calculating the Richardson Number in numerically simulated storms, and then show that the assumption of constant Richardson Number determines the variation of the outflow temperature with angular momentum or entropy and thereby sets the radial structure of the storm outside its radius of maximum surface winds. In Part II we will show that allowing the outflow temperature to vary also allows one to discard an empirical factor that was introduced in previous work on the intensification of tropical cyclones.

[1] The National Center for Atmospheric Research is sponsored by the National Science Foundation

## 1. Introduction

The nearly circular symmetry of mature tropical cyclones, together with the observation that they can exist in a quasi-steady state for some time, provides an opportunity for relatively simple description of their physics and structure. Further assumptions of hydrostatic and gradient wind balance and convective neutrality of the vortex lead to strong constraints on its intensity and structure, as elucidated by Kleinschmidt (1951), Lilly (unpublished manuscript, 1973), Shutts (1981), and Emanuel (1986), among others. When coupled with formulas for surface fluxes of enthalpy and momentum, the radial distribution of boundary layer gradient wind is given as a function of the local air-sea enthalpy disequilibrium, the difference in absolute temperature between the top of the boundary layer and the outflow level, and nondimensional surface exchange coefficients.

One issue that arises in constructing solutions of this kind is the specification of the so called "outflow temperature" – the absolute temperature attained by streamlines flowing upward and outward from the storm's core as they asymptotically level out at large radii. Lilly (unpublished manuscript, 1973) and Emanuel (1986) both assumed that a streamline emanating from the storm's core would asymptote to the unperturbed environmental isentropic surface whose entropy matches that of the streamline, under the assumption that the vortex is "subcritical", i.e. that internal waves are fast enough to propagate from the environment inward against the outflow, so that the structure of the core is, in effect, partially determined by the unperturbed environmental entropy stratification. In developing solutions to the interior equations, Lilly assumed that the upper tropical troposphere has sub-moist adiabatic lapse rates, so that entropy is increasing upward, and that therefore, the outflow would be in the upper troposphere, with outflow temperature increasing with decreasing entropy. By contrast, Emanuel (1986) regarded the whole ambient troposphere as being neutral to moist convection, so that any streamline reflecting elevated boundary layer entropy would have to flow out of the storm at levels above the tropopause. Since the temperature structure of the atmosphere above the tropopause is approximately isothermal, Emanuel approximated the outflow temperature as a constant. (Shutts (1981) arbitrarily specified the radial profile of gradient wind in the vortex and determined outflow temperature that was consistent with such a profile.)

Whichever assumption is used, the radial structure of the solutions is sensitive to the dependence of outflow temperature on the entropy of the outflowing streamlines. In particular, the assumption of constant outflow temperature leads to a highly unrealistic radial profile of gradient wind, unless additional assumptions are made about the entropy budget of the boundary layer, as in Emanuel (1986). Moreover, attempts to find time-dependent solutions under the assumption of constant outflow temperature lead to the conclusion that all nascent vortices should decay with time, unless an empirical factor is introduced that keeps the boundary layer entropy low outside the storm's core (Emanuel, 1997).

The poor solutions that result when constant outflow temperature is assumed, together with the great sensitivity of the solutions to the stratification of the upper troposphere when it is assumed to be positive, motivate a re-examination of the problem. After reviewing the steady-state theory, we begin by examining the structure of the outflow in a tropical cyclone simulated using a convection-resolving

axisymmetric model, and show that the outflow attains an entropy stratification that appears to be independent of any small stratification that may be present in the unperturbed environment. We then postulate that this stratification arises from small scale turbulence and tends toward a value consistent with the hypothesis that the Richardson Number is near a critical value. We test this hypothesis using data generated by the numerical simulations, and proceed to examine its implications for the structure and intensification of the vortex. The paper concludes with a brief summary.

## 2. Review of analytic axisymmetric models

Analytical models of steady, axisymmetric vortices date back to Lilly (unpublished manuscript, 1973), Shutts (1981), and Emanuel (1986). The most sophisticated of these, developed originally by Lilly, is based on conservation of energy, entropy, and angular momentum above the boundary layer, and is reviewed in Bister and Emanuel (1998) and Emanuel (2004). It makes no assumption about hydrostatic or gradient balance above the boundary layer but is difficult to solve. For this reason, and because real and numerically simulated tropical cyclones are observed to be nearly in hydrostatic and gradient wind balance above the boundary layer, we follow Emanuel (1986) in assuming that such balances apply and further that the saturation entropy above the boundary layer does not vary along surfaces of constant absolute angular momentum. Where air is flowing upward out of the boundary layer, it is likely to be saturated and the coincidence of entropy and angular momentum surfaces is then demanded by conservation of both quantities. Here and elsewhere in the vortex this state is also the condition for neutrality to slantwise moist convection (Emanuel, 1983). Saturation entropy is defined

$$s^* = c_p \ln T - R_d \ln p + \frac{L_v q^*}{T}, \tag{1}$$

where $T$ is the absolute temperature, $p$ the pressure, $q^*$ the saturation specific humidity, $c_p$ the heat capacity at constant pressure, $R_d$ the gas constant of dry air, and $L_v$ the latent heat of vaporization. In (1) we have neglected the small effect of condensed water on heat capacity and the gas constant. Absolute angular momentum per unit mass is defined

$$M = rV + \frac{1}{2} fr^2, \tag{2}$$

where $V$ is the azimuthal velocity, $r$ the radius, and $f$ the Coriolis parameter.

The condition that $s^*$ is a function of $M$ alone, together with hydrostatic and gradient wind balance, places strong constraints on the structure of the vortex. This can be seen by integrating the thermal wind equation along angular momentum surfaces. To develop an appropriate form of the thermal wind equation, we begin by writing the equations of hydrostatic and gradient balance in pressure coordinates:

$$\frac{\partial \phi}{\partial p} = -\alpha, \tag{3}$$

and

$$\frac{\partial \phi}{\partial r} = \frac{V^2}{r} + fV = \frac{M^2}{r^3} - \frac{1}{4} f^2 r. \tag{4}$$

Here $\alpha$ is the specific volume, $\phi$ is the geopotential, and its gradient with respect to $r$ in (4) is taken holding pressure constant. The thermal wind equation is obtained by differentiating (3) with respect to $r$ and subtracting the derivative of (4) with respect to $p$ to obtain

$$\frac{1}{r^3}\frac{\partial M^2}{\partial p} = -\frac{\partial \alpha}{\partial r}. \tag{5}$$

Since $s^*$ is a state variable, we may express the specific volume $\alpha$ as a function of it and of pressure,[2] $p$ , so that by the chain rule, (5) becomes

$$\frac{1}{r^3}\frac{\partial M^2}{\partial p} = -\frac{\partial \alpha}{\partial s^*}\frac{\partial s^*}{\partial r}. \tag{6}$$

Using one of Maxwell's relations (Emanuel, 1986)

$$\left(\frac{\partial \alpha}{\partial s^*}\right)_p = \left(\frac{\partial T}{\partial p}\right)_{s^*},$$

we may write (6) as

$$\frac{1}{r^3}\frac{\partial M^2}{\partial p} = -\left(\frac{\partial T}{\partial p}\right)_{s^*}\frac{\partial s^*}{\partial r}. \tag{7}$$

But $s^*$ is a function of $M$ alone in a slantwise neutral vortex, so (7) can be rewritten

$$\frac{1}{r^3}\frac{\partial M^2}{\partial p} = -\left(\frac{\partial T}{\partial p}\right)_{s^*}\frac{ds^*}{dM}\frac{\partial M}{\partial r}. \tag{8}$$

Dividing each side of (8) by $\partial M / \partial r$ yields an equation for the slope of angular momentum surfaces:

$$\frac{2}{r^3}\left(\frac{\partial r}{\partial p}\right)_M = \left(\frac{\partial T}{\partial p}\right)_{s^*}\frac{1}{M}\frac{ds^*}{dM} \tag{9}$$

Since neither $M$ nor $ds^*/dM$ vary on angular momentum surfaces, (9) may be directly integrated in pressure to yield

[2] Here we are neglecting the direct effect of the presence of water substance on specific volume.

$$\frac{1}{r_b^2} = \frac{1}{r^2} - (T_b - T)\frac{1}{M}\frac{ds*}{dM}, \tag{10}$$

where $r_b$ and $T_b$ are the radius and temperature where a given angular momentum surface intersects the top of the boundary layer. Multiplying (10) through by $M$ and using its definition (2) yields

$$\frac{V_b}{r_b} = \frac{V}{r} - (T_b - T)\frac{ds*}{dM}, \tag{11}$$

where $V_b$ is the azimuthal velocity where the angular momentum surface in question intersects the top of the boundary layer.

The form of (11) suggests two possible definitions of "outflow temperature". The first is to define it as the temperature along an angular momentum surface where is passes through the locus of points defined by $V = 0$ . In that case, (11) may be written

$$\frac{V_b}{r_b} = -(T_b - T_o)\frac{ds*}{dM}, \tag{12}$$

where $T_o$ is the outflow temperature thus defined. A second choice is to define the outflow temperature as the temperature along an angular momentum surface in the limit as $r \to \infty$ . In that case, from (11) and using $V = M/r - 1/2\, fr$ , we have

$$\frac{V_b}{r_b} = -\frac{1}{2} f - (T_b - T_o)\frac{ds*}{dM}. \tag{13}$$

For angular momentum surfaces originating near the storm's core, where $V/r >> f$ , the two definitions of outflow temperature leading to (12) and (13) yield almost identical results. Either way, one should think of $T_o$ as an upper or outer boundary condition, and note that it may be a function of $s$*, $M$, or streamfunction.

The relation (12) or (13) yields the distribution of angular velocity at the top of the boundary layer provided that $s*$ is a known function of $M$ and that the outflow temperature $T_o$ is a known function of $s*$ (or $M$ ). Lilly, Emanuel (1986), and subsequent papers argued that the function $ds*/dM$ is determined by the boundary layer entropy and angular momentum balance. In particular, neutrality to moist convection requires that the saturation entropy above the lifted condensation level equal the actual entropy, $s$ , of the boundary layer. The budget equation for boundary layer entropy, written in angular momentum – pressure coordinates and neglecting dissipative heating, is

$$\frac{\partial s}{\partial \tau} + \dot{M}\frac{\partial s}{\partial M} + \omega\frac{\partial s}{\partial p} = -g\frac{\partial F}{\partial p}, \tag{14}$$

where $\dot{M}$ is the total time derivative of angular momentum and $F$ is the vertical turbulent flux of entropy. The former may be derived from the azimuthal momentum equation:

$$\dot{M} = -gr\frac{\partial \tau_\theta}{\partial p}, \tag{15}$$

where $\tau_\theta$ is the tangential stress. Substituting (15) into (14) and assuming a steady state yields

$$-gr\frac{\partial \tau_\theta}{\partial p}\frac{\partial s}{\partial M} + \omega\frac{\partial s}{\partial p} = -g\frac{\partial F}{\partial p}. \tag{16}$$

We now make two important assumptions about the distributions of entropy and angular momentum in the turbulent boundary layer. The first is that entropy is well mixed along angular momentum surfaces, which are approximately vertical in the boundary layer, so that the second term on the left of (16) is nearly zero while at the same time $\partial s / \partial M \cong ds / dM$ is not a function of pressure. The second assumption is that the radius of angular momentum surfaces does not vary greatly with altitude within the boundary layer. To the extent these two approximations hold[3], (16) may be integrated through the depth of the boundary layer to yield

$$\frac{ds}{dM} = \frac{F_s}{\overline{r}\tau_{\theta s}}, \tag{17}$$

where $F_s$ is the surface entropy flux[4], $\tau_{\theta s}$ is the surface azimuthal stress, $\overline{r}$ is the vertically averaged radius of angular momentum surfaces, weighted by the convergence of the turbulent flux of momentum, and we have defined the top of the boundary layer as the level at which the turbulent fluxes of entropy and momentum vanish. Bryan and Rotunno (2009a) showed that (17) is well satisfied in numerical simulations. Substitution of (17) into (12) yields

$$\frac{\overline{r}}{r_b}V_b = -(T_b - T_o)\frac{F_s}{\tau_{\theta s}} \tag{18}$$

Thus if the surface fluxes of momentum and enthalpy are known, if the outflow temperature is a known function of entropy, and if one can relate $\overline{r}$ to $r_b$, the gradient wind at the top of the boundary layer, $V_b$, can be found.

[3] Note that we have not at this point assumed anything about gradient wind balance in the boundary layer, contrary to the assertion of Smith et al. (2008).

[4] Formally, the surface enthalpy flux divided by the surface temperature.

To close the problem, we need to formulate surface fluxes in terms of known variables and to say something about the outflow temperature. For surface fluxes, we use the classical aerodynamic flux formulae[5]:

$$F_s = \frac{C_k \rho \,|\mathbf{V}|\left(k_0^* - k\right)}{T_s}, \tag{19}$$

$$\tau_{\theta s} = -C_D \rho \,|\mathbf{V}| V, \tag{20}$$

where $C_k$ and $C_D$ are dimensionless exchange coefficients for enthalpy and momentum, $\rho$ is the air density, $|\mathbf{V}|$ is the wind speed, $k_0^*$ is the saturation enthalpy of the sea surface, $k$ is the actual enthalpy of air at the reference level at which the wind speed and exchange coefficients are defined, and $T_s$ is the sea surface temperature. Using (19) and (20) in 18 gives

$$\frac{\overline{r}}{r_b} V V_b = \frac{C_k}{C_D}(T_b - T_o)\frac{\left(k_0^* - k\right)}{T_s}. \tag{21}$$

Note that the wind speed at the flux reference level, $|\mathbf{V}|$, has dropped out.

It has become traditional to make several more approximations in (21), and we pause here to examine their credibility. First, we might approximate the azimuthal wind at the reference level, $V$, by the gradient wind $V_b$. As pointed out by Smith et al. (2008) and others, this may not be a very good approximation, especially near the radius of maximum winds, where the wind speed may appreciably exceed its gradient value. Let us suppose, for the sake of argument, that $V$ exceeds $V_b$ by 30%. Making the approximation that $V = V_b$ in (21) would then yield an error of about 15%, owing to the fact that one is taking the square root of the right-hand side of (21). But in reality the error would not be that large, owing to a compensation that occurs in the first factor on the left of (21), $\overline{r} / r_b$. When the actual wind is supergradient, $\overline{r} < r_b$, and this works to compensate the fact that $V > V_b$ in (21). (In the special case that $\overline{r}$ is the radius of the angular momentum surface where it passes through the flux reference level, the compensation is exact.) Thus if we make both of the two approximations $\overline{r} \cong r_b$ and $V \cong V_b$ in (21), we can write an approximate equation for the gradient wind that is likely to be in error by less than 10%:

$$V_b^2 \cong \frac{C_k}{C_D}(T_b - T_o)\frac{\left(k_0^* - k\right)}{T_s}. \tag{22}$$

We emphasize that this is a relation for the gradient wind, and not the actual wind in the boundary layer, which, as noted above, can appreciably exceed its gradient value near the radius of maximum

[5] But note that under hurricane-force winds, these may not be appropriate. On the other hand, they are used in the numerical simulations against which we will test the theory.

winds. We should also point out that the specification of $V_b$ as a function of radius would allow a complete calculation of the actual boundary layer wind were it used to drive a complete boundary layer model, as in Kepert (2010). We also note that were dissipative heating included in the derivation of (22), then as shown by Bister and Emanuel (1998), the surface temperature $T_s$ that appears in (22) would be replaced by the outflow temperature, $T_o$.

The relation given by (22) is still not a closed solution for the gradient wind, because a) the enthalpy in the boundary layer, $k$, is not known *a priori*, and b) the outflow temperature must be specified. The first problem can be addressed by integrating (17) inward from some specified outer radius, using (19) and (20) to specify the surface fluxes and with the gradient wind specified along the way by solving (22) and using a thermodynamic relationship between enthalpy and entropy. But this procedure also requires knowledge of $T_o$ as a function of entropy or angular momentum. It is the problem of that specification that we address here.

## 3. The outflow temperature

As mentioned in the Introduction, previous work has treated hurricane outflow as subcritical, in the sense that internal waves can propagate inward against the outflow and thereby transmit information from the environment inward to the core. It was assumed that this subcriticality would ensure a match between the entropy stratification of the outflow and that of the unperturbed environment: Air flowing out of the core would attain an altitude such that its saturation entropy matched that of the distant environment. Lilly assumed that the upper tropical troposphere has a temperature lapse rate less than moist adiabatic, so that moist entropy would be increasing with altitude, and the outflow would therefore be mostly or entirely in the upper troposphere. Emanuel (1986) and subsequent work assumed that the whole tropical troposphere is nearly neutral to moist convection and thus would have nearly constant saturation entropy; boundary layer air with entropy larger than that of the unperturbed environment would therefore have to flow out of the storm above the level of the unperturbed tropopause. Since the absolute temperature can be nearly constant with height just above the tropopause, one could assume constant outflow temperature as a first approximation.

But consider the consequences of constant outflow temperature for the radial structure of the gradient wind as given by (22). Since the quantity $k_0^* - k$ usually increases monotonically with radius, then $V$ would therefore also have to increase monotonically with radius, which of course does not happen. Emanuel (1986) and subsequent work addressed this obvious problem by postulating that outside the storm's core, turbulent fluxes of entropy out of the top of the boundary layer keep the boundary layer entropy relatively low and invalidate (17) in that region. This idea is supported qualitatively by the boundary layer entropy budget of a cloud-resolving, axisymmetric model simulation by Rotunno and Emanuel (1987)(hereafter RE87), which showed that outside the core, surface enthalpy fluxes are balanced mostly by convective fluxes out of the top of the boundary layer. On the other hand, the recent successful simulation of a completely dry hurricane by Smith-Mrowiec et al. (personal

communication) calls into question whether the import of low entropy air to the boundary layer by convective downdrafts is really essential to hurricane physics.

The poor prediction of the radial structure of the gradient wind by (22) with constant $T_o$ motivates us to re-examine the question of outflow temperature. We begin by carrying out a numerical simulation of a tropical cyclone using a nonhydrostatic, convection-permitting axisymmetric model. The model is that of RE87 modified so that the finite difference equations conserve energy. The model is run on a uniform grid in the radius-altitude plane, with radial and vertical grid spacings of 3.75 km and 312.5 m, respectively, in a domain extending to 1500 km in radius and 25 km in altitude. The Coriolis parameter is set to $5\times10^{-5}\ s^{-1}$. To better compare with the theory developed in section 4, we here omit dissipative heating as well as the pressure dependence of the sea surface potential temperature and saturation specific humidity, so that the surface saturation entropy is constant. In RE87, the vertical mixing length was 200 m but here we set it to 1000 m. Experiments with smaller vertical mixing lengths show only a weak dependence of storm structure and peak wind speed, but the effect we wish to illustrate here was more clearly defined for the larger mixing length. Also, the surface exchange coefficients, which depend on wind speed, are both capped at $3\times10^{-3}$, but they approach this value at a faster rate of $6\times10^{-5}\left(m/s\right)^{-1}$. All other parameters are set to the values listed in Table 1 of RE87.

The initial atmospheric temperature is specified to lie along a pseudo-moist adiabat from the lifted condensation level of air at the lowest model level to a tropopause at an altitude just below 15 km and having a temperature of -86.7 C. For simplicity, the stratosphere is initially isothermal, having the same temperature as the tropopause. The sounding is dry adiabatic from the sea surface to the lifted condensation level, and the sea surface temperature is held constant at $24.89\ \mathrm{C}$, yielding a potential intensity calculated using the algorithm described by Bister and Emanuel (2002), but with the sea surface saturation enthalpy held constant, of $67.9\ ms^{-1}$. The initial sounding is shown in Figure 1.

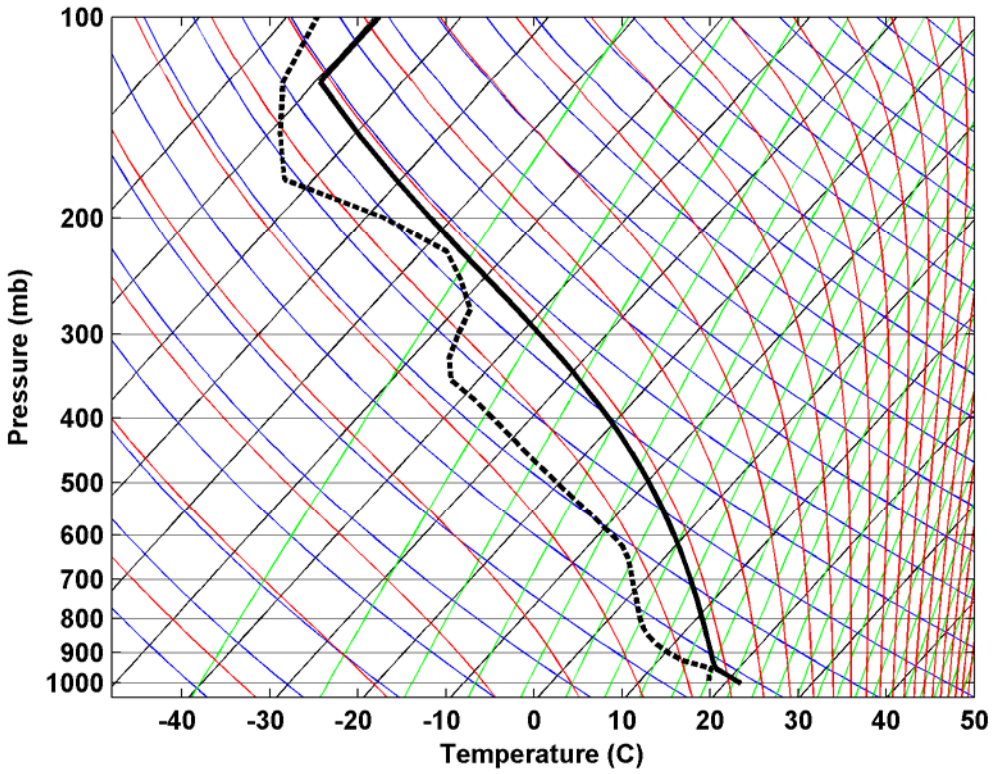


**Figure 1: Initial sounding used in simulations with an updated version of the RE87 numerical model. Temperature plotted in black; dashed line shows dew point temperature.**

The simulation is initialized with a weak, warm-core vortex and is integrated forward in time until a quasi-steady state is achieved. The time evolution of the maximum wind in the model domain as well as the maximum wind at the lowest model level is shown in Figure 2 and compared to the aforementioned theoretical potential intensity. As shown by Bryan and Rotunno (2009b), the intensity achieved in such simulations is usually close to the theoretical potential intensity if the horizontal mixing length is sufficiently large, as it is here. For smaller mixing lengths, the actual boundary layer wind can be appreciably larger than its gradient value near the radius of maximum winds. While the existence of supergradient winds is clearly of interest, our purpose here is to focus on those deficiencies of the existing theory that are related to outflow temperature, thus we choose to examine a simulation that does not otherwise exhibit serious discrepancies with theory.

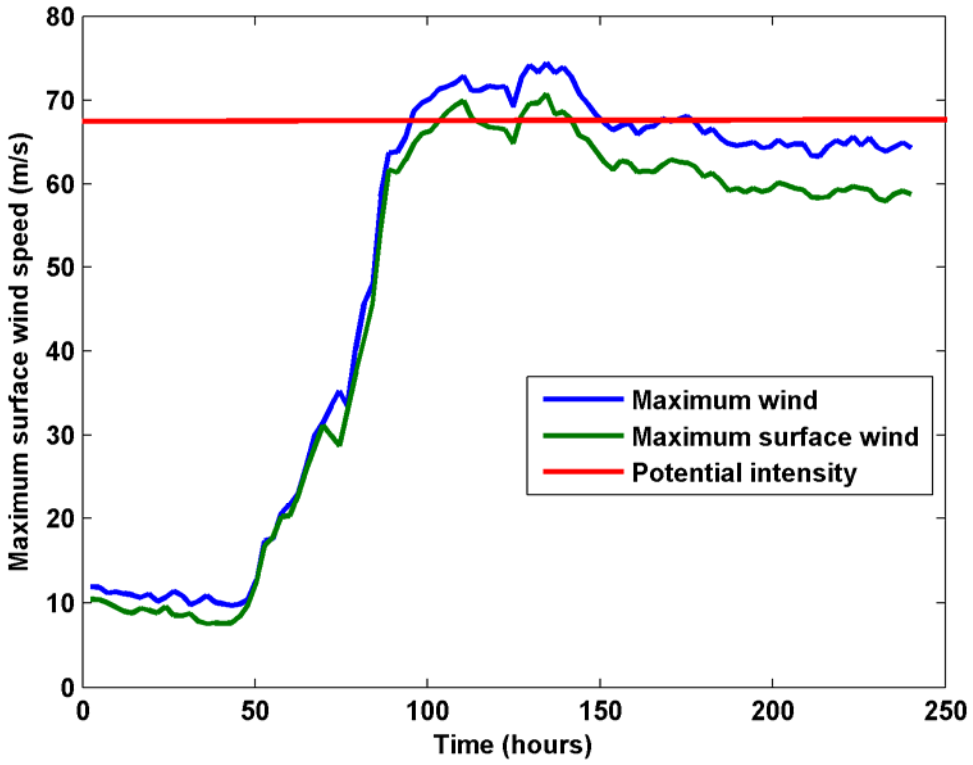


**Figure 2: Evolution with time of the peak wind speed (m/s) at the lowest model level (green) and within the whole domain (blue) in a simulation using an updated version of the RE87 model.**

Figure 3 shows the distribution in the radius-altitude plane of saturation equivalent potential temperature averaged over the last 24 hours of the integration, together with the contour representing the loci of vanishing azimuthal wind, likewise averaged over 24 hours. We note several features of interest. First, it is clear that while some of the contours of saturation equivalent potential temperature erupting from the boundary layer near the radius of maximum winds (about 34 km) intersect the $V = 0$ contour above the altitude of the ambient tropopause (also shown in Figure 3), many such surfaces erupting outside the radius of maximum winds flow out below the ambient tropopause. Moreover, the stratification of saturation equivalent potential temperature near the $V = 0$ contour does not seem to be related in any obvious way to the ambient stratification, which is zero below the tropopause and large and nearly constant above it; thus we regard the outflow as *self stratifying*. Figure 4 shows the mass streamfunction averaged over the final 24 hours of the integration, together with the $V = 0$ contour; clearly, much of the outflow is below the tropopause and the absolute temperature increases monotonically with the value of the streamfunction, and with decreasing saturation entropy. Remember that, according to (12), the outflow temperature is defined as the temperature at which saturation entropy (or angular momentum) surfaces pass through the $V = 0$ contour.

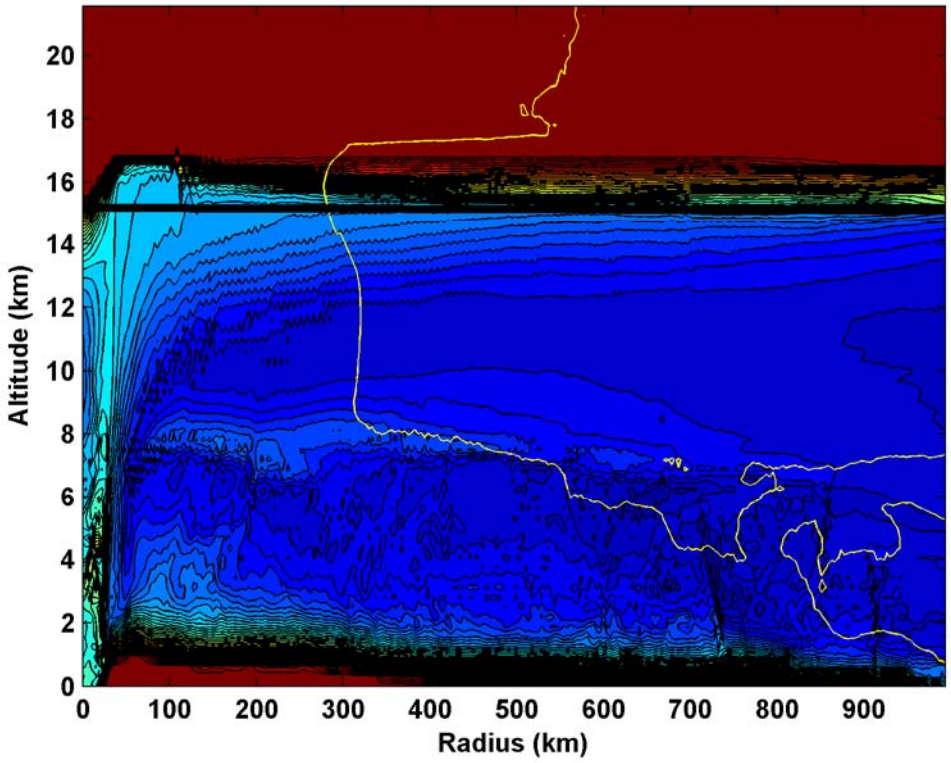


**Figure 3: Distribution in the radius-altitude plane of saturation equivalent potential temperature averaged over the last 24 hours of the numerical simulation described in the text. The yellow curve represents the $V = 0$ contour and the thick black line represents the altitude of the ambient tropopause. For clarity, values of saturation equivalent potential temperature have been capped at 385 K.**

The supposition that the outflow temperature increases with angular momentum is borne out by interpolating absolute temperature onto angular momentum surfaces. Figure 5 traces the changes in absolute temperature and azimuthal velocity along each of a family of angular momentum surfaces separated by equal increments of angular momentum. The surfaces span roughly the interval between the radius of maximum surface wind and the radius of gale-force winds. The angular momentum surfaces fall into two groups: The left-most group, representing relatively small values of angular momentum, are surfaces along which the mean flow is upward while the right-most group consists of angular momentum surfaces along which the mean flow is directed downward. In between and above the boundary layer is a region of nearly constant angular momentum. The red curve in Figure 5 shows the solution to (10) with (17) for the conditions of this simulation; clearly the angular momentum surface originating from the radius of maximum winds is close to that given by thermal wind balance above the boundary layer.

From Figure 5, it is clear that within the upflow, outflow temperature increases with angular momentum; slowly at first and then more rapidly as angular momentum increases. The outflow temperature of the angular momentum surface erupting at the radius of maximum surface wind is very close to the ambient tropopause temperature in this simulation, but the assumption of constant outflow

temperature for angular momentum surfaces originating outside the radius of maximum winds is poor. And, since in this simulation the ambient atmosphere above the tropopause is isothermal while there is no stratification of saturation entropy below the tropopause, one cannot assume that the outflow streamlines asymptote to absolute temperatures corresponding to those of undisturbed saturation entropy surfaces of the environment. (Doing so for this simulation would yield a constant outflow temperature.)

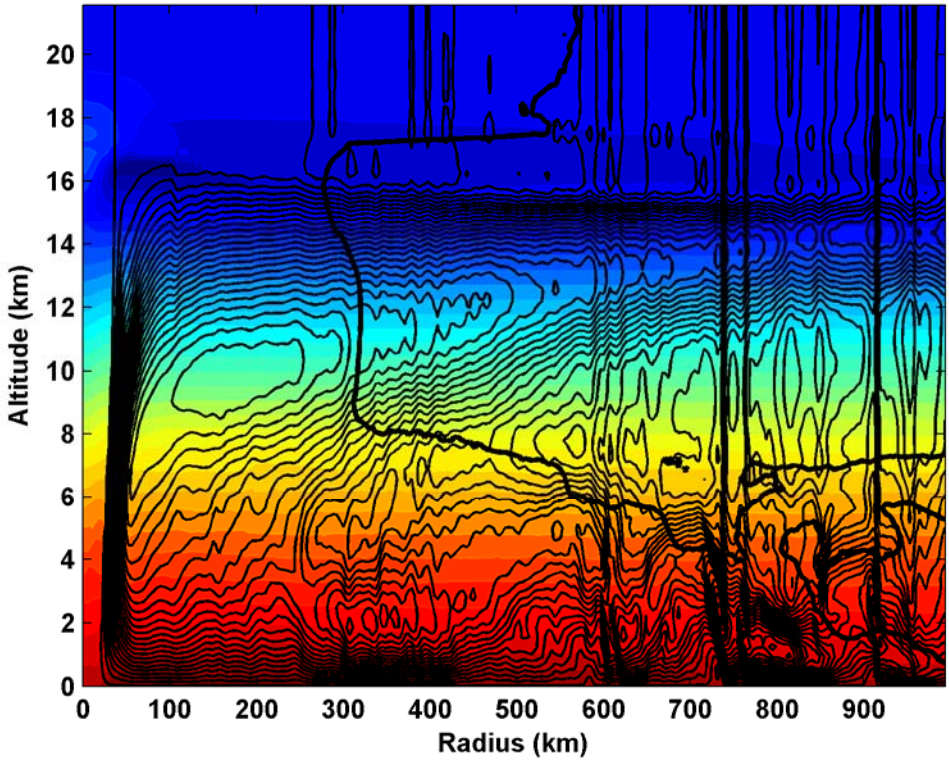


**Figure 4: Mass streamfunction (black contours) and absolute temperature (K; colors) averaged over the last 24 hours of the simulation described in the text. The thick black contour represents $V = 0$ .**

Figure 5 presents strong evidence that hurricane outflow is self-stratifying, at least when the ambient upper troposphere has a moist adiabatic lapse rate. But what determines the stratification of the outflow? Specification of the dependence of outflow temperature on saturation entropy (or angular momentum) is sufficient to determine the radial profile of gradient wind in the boundary layer through (22); conversely, if one had an independent means of specifying the radial profile of boundary layer gradient wind, then the outflow temperature would be determined by (22). As we can think of no independent principle to determine the radial profile of gradient wind, we focus our attention on physical constraints on the outflow stratification.

Consider what would happen if all of the outflow streamlines asymptotically approached environmental isentropic surfaces corresponding to their own values of entropy, as originally postulated. Then, referring to Figure 3, there would be large gradients of saturation entropy, angular

momentum, and streamfunction in the outflow. The Richardson Number ( $Ri$ ) would be small, suggesting that small scale turbulence would occur, mixing velocity and entropy and thereby expanding the depth of the outflow. Such an outcome is also possible in our numerical simulation, since the subgrid-scale turbulence parameterization of RE87 is sensitive to $Ri$ . It is also possible that horizontal mixing in the upflow contributes to the physical spacing of angular momentum and entropy surfaces.

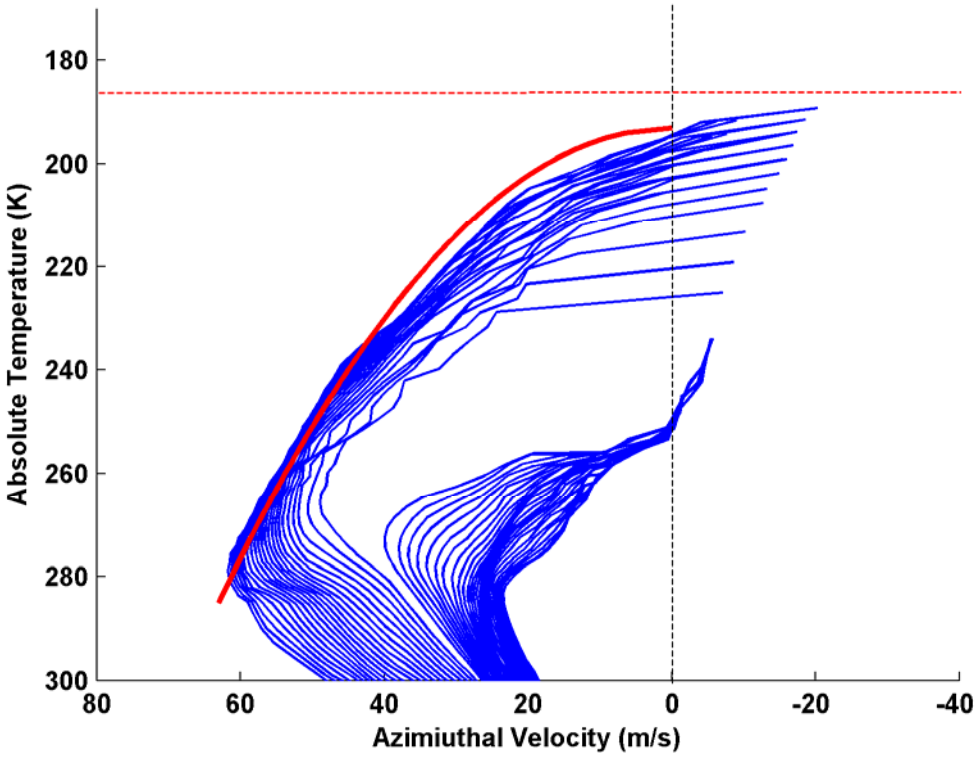


**Figure 5: Family of surfaces (blue) of constant absolute angular momentum traced versus absolute temperature and azimuthal velocity. The solid red curve shows the shape of the angular momentum intersecting the boundary layer top at the radius of maximum winds, calculated assuming thermal wind balance. The dashed black line represents vanishing azimuthal wind, while the dashed red line shows the ambient tropopause temperature. The inner most angular momentum surface originates near the radius of maximum wind.**

The distribution of $\sqrt{Ri}$ calculated from fields averaged over the last 24 hours of the simulation is shown in Figure 6. Here $Ri$ is defined

$$Ri \equiv \frac{\Gamma_m \dfrac{\partial s^*}{\partial z}}{\left(\dfrac{\partial U}{\partial z}\right)^2 + \left(\dfrac{\partial V}{\partial z}\right)^2}, \tag{23}$$

where $\Gamma_m$ is the moist adiabatic lapse rate and $U$ is the radial velocity. In the region where the eyewall upflow turns outward, becoming outflow, $Ri$ is relatively small. Figure 7 shows a scatter plot of the numerator of (23) against the denominator, for a region bounded by the black box shown in Figure 6.

The value of $Ri$ seldom falls below about 1, which is shown by the black line in the figure. The critical value of $Ri$ for the onset of turbulence in the RE87 model is 1, but several aspects of the computation performed here may distort the calculated value of $Ri$. First, we have neglected the contribution to $Ri$ of vertical gradients in condensed water content, as it appears in eq. (28) of RE87. Second, we have calculated $Ri$ from the time-averaged wind and entropy fields rather than taking the time average of the instantaneous values of $Ri$. Nevertheless, Figure 6 shows that $Ri$ may be systematically limited by a

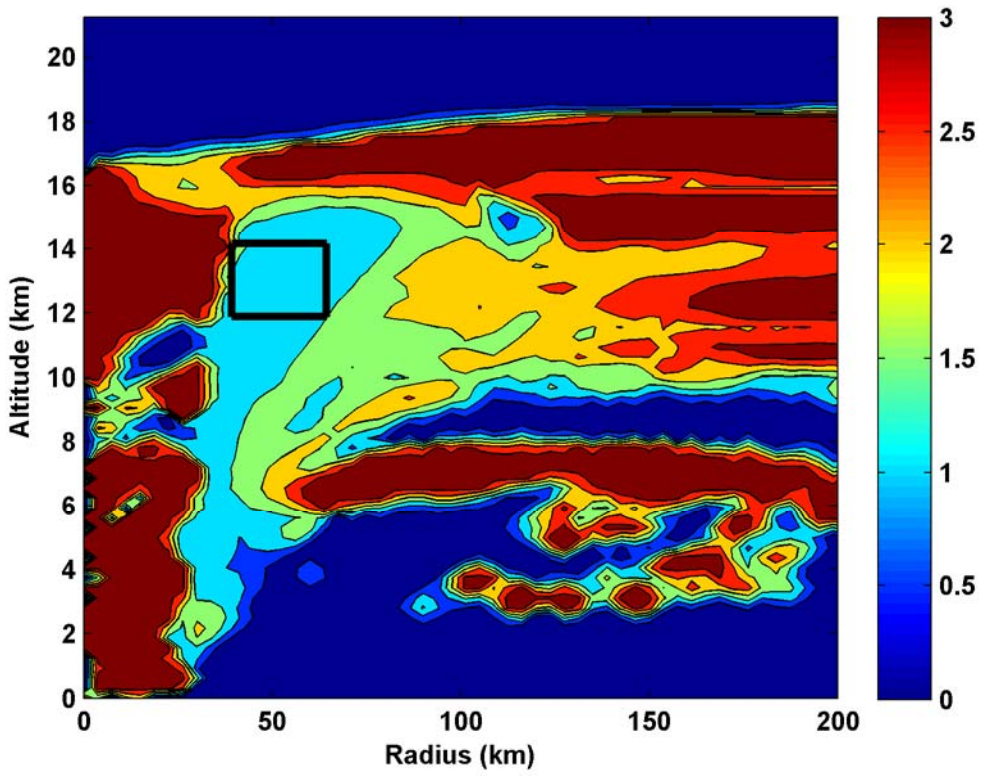


**Figure 6: Square root of the Richardson number calculated from flow fields averaged over the last 24 hours of the simulation described in the text. Values are bounded below by zero and above be three. The small black box shows the region from which the data plotted in figure 7 are drawn.**

critical value in some region of the storm's outflow. We can now show that this region is likely to be in the eyewall. First, we neglect $\partial U / \partial z$ compared to $\partial V / \partial z$ in the denominator of (23), and substitute

$$\frac{\partial V}{\partial z} = \frac{1}{r}\frac{\partial M}{\partial z}.$$

Since $s*$ is a function of $M$ alone,

$$\frac{\partial s*}{\partial z} = \frac{ds*}{dM}\frac{\partial M}{\partial z}.$$

Using these in (23) gives

$$Ri \cong \frac{r^2 \Gamma_m \dfrac{ds*}{dM}}{\dfrac{\partial M}{\partial z}}. \qquad (24)$$

Thus, along any given streamline, $Ri$ will be small at small radius and where $\partial M / \partial z$ is large. This corresponds well with the location of the box in Figure 6. In the following sections, we will explore the implications of the hypothesis of critical Richardson Number for the structure and intensification of tropical cyclones.

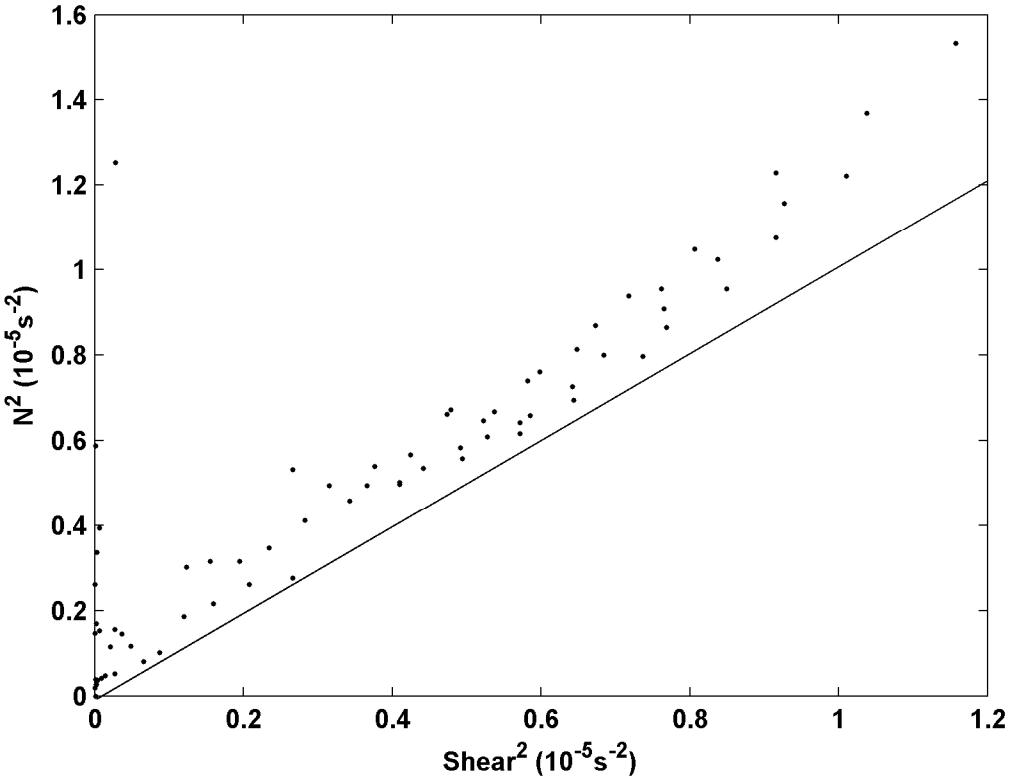


**Figure 7: The buoyancy frequency squared plotted against the square of the vertical shear of the horizontal wind calculated from quantities averaged over the last 24 hours of the simulation described in the text. The data are drawn from the region shown by the black box in Figure 6. The straight black line corresponds to a Richardson Number of 1.**

## 4. Implications of critical Richardson Number for steady-state structure

Suppose that the Richardson Number is held to be at some fixed, critical value $Ri_c$ at some radius, $r_t$. Then (24) implies that

$$\frac{\partial M}{\partial z} \cong \frac{r_t^2 \Gamma_m \frac{ds*}{dM}}{Ri_c}. \tag{25}$$

Using

$$\frac{\partial s*}{\partial z} = \frac{ds*}{dM}\frac{\partial M}{\partial z},$$

we can write (25) as

$$\frac{\partial s*}{\partial z} \cong \frac{r_t^2 \Gamma_m \left(\frac{ds*}{dM}\right)^2}{Ri_c}. \tag{26}$$

Thus the assumption of critical Richardson number at some radius $r_t$ constrains the vertical gradient of saturation entropy there. But since $s*$ is a state variable, its vertical gradient dictates the vertical gradient of temperature, from which one can deduce the gradient of temperature with respect to $s*$. Using the chain rule, we first write

$$\frac{\partial T}{\partial s*} = \left(\frac{\partial T}{\partial s*}\right)_p + \frac{\left(\frac{\partial T}{\partial p}\right)_{s*}}{\frac{\partial s*}{\partial p}}, \tag{27}$$

where the subscripts denote the quantity being held constant. Using the definition of saturation entropy and the Clausius-Clapeyron equation, we can write the first term

$$\left(\frac{\partial T}{\partial s*}\right)_p = \frac{\frac{T}{c_p}}{\left[1 + \frac{L_v^2 q*}{R_v c_p T^2}\right]}, \tag{28}$$

where $c_p$ is the heat capacity at constant pressure, $L_v$ the latent heat of vaporization, $q*$ the saturation specific humidity, and $R_v$ the gas constant for water vapor. Using the hydrostatic approximation for the second term in (27) and substituting (28), (27) can be written

$$\frac{\partial T}{\partial s^*} = \frac{\dfrac{T}{c_p}}{\left[1 + \dfrac{L_v^2 q^*}{R_v c_p T^2}\right]} - \frac{\Gamma_m}{\dfrac{\partial s^*}{\partial z}}. \tag{29}$$

For vertical gradients of $s^*$ that are consistent with (26), the second term on the right side of (29) is roughly an order-of-magnitude greater than the first. Using this approximation and substituting (26) into (29) gives

$$\frac{\partial T}{\partial s^*} \cong -\frac{Ri_c}{r_t^2}\left(\frac{dM}{ds^*}\right)^2. \tag{30}$$

This yields the dependence of outflow temperature on saturation entropy consistent with the critical Richardson number hypothesis. Although this applies to the region where the Richardson Number is near its critical value, we assume (30) also approximates the dependence of outflow temperature on saturation entropy. Using

$$\frac{\partial T}{\partial s^*} = \frac{\partial T}{\partial M}\frac{dM}{ds^*},$$

we may write (30) alternatively as

$$\frac{\partial T}{\partial M} \cong -\frac{Ri_c}{r_t^2}\left(\frac{dM}{ds^*}\right). \tag{31}$$

This will allow us to solve for the outflow temperature in angular momentum coordinates.

A complete model for the steady-state structure of a tropical cyclone whose outflow temperature is specified by (31) may now be formulated. We begin with the definition of angular momentum, given by (2), and substitute (12) for the gradient wind at the top of the boundary layer:

$$M_b = r_b^2\left(\frac{1}{2} f - \left(T_b - T\right)\frac{ds^*}{dM}\right), \tag{32}$$

where $M_b$ is the angular momentum at the top of the boundary layer. Substituting (19) and (20) into (17) and making use of (12) gives

$$\left(\frac{ds^*}{dM}\right)^2 = \frac{C_k}{C_d}\frac{s_0^* - s^*}{r_b^2\left(T_b - T\right)}, \tag{33}$$

in which we have also used the approximation

$$\frac{k_0^* - k}{T_s} \cong s_0^* - s^*,$$

where $s_0$* is the saturation entropy of the sea surface and we have equated the boundary layer entropy with the saturation entropy of the free troposphere. Eliminating $r_b^2$ between (32) and (33) gives a quadratic equation for $ds*/dM$ :

$$\left(\frac{ds*}{dM}\right)^2 + 2\chi\frac{ds*}{dM} - \frac{\chi f}{T_b - T} = 0, \tag{34}$$

where

$$\chi \equiv \frac{C_k}{C_D}\frac{s_0* - s*}{2M}.$$

The physically relevant solution to (34) is

$$\frac{ds*}{dM} = -\chi - \sqrt{\chi^2 + \frac{\chi f}{T_b - T}}. \tag{35}$$

Starting from some outer angular momentum surface, $M_o$ , (35) and (31) can be marched inward to yield $s*$ and $T$ as functions of $M$ . Once these quantities have been obtained, $r_b$ can be found using (32) and then the gradient wind can be found from the definition of angular momentum, (2). One complication is that $s_0$* depends on pressure, so that, in principle, one should also march the gradient wind equation inward to find the local surface pressure. For simplicity, we take $s_0$* to be a specified constant here. A more serious problem is that the condition of Richardson Number criticality may not apply to the region of downflow, which for the aforementioned numerical simulation begins at about 120 km from the storm center. We shall return to this problem presently.

One must also satisfy boundary conditions. Given that (31) and (35) are first-order differential equations, two boundary conditions must be specified. The first might be to require the gradient wind to vanish at some outer radius, $r_o$ . Marching (35) inward will result in a monotonic increase in $s*$, which will eventually reduce $\chi$ in spite of decreasing $M$ . Thus, according to (22), the gradient wind will achieve a maximum value at some particular value of $M$ . On the other hand, the outflow temperature should achieve the ambient tropopause temperature, $T_o$ , at or near the radius of maximum winds, but there is no guarantee from integrating (31) that this will be so. Thus, a "shooting" method is applied in which an outer radius is first specified, the system integrated, and the outflow temperature at the radius of maximum winds is noted. If it is not equal to $T_o$ , the integration is restarted with e new value of $r_o$ , and so on, until the outflow temperature at the radius of maximum winds equals $T_o$ . Alternatively, one could simply specify the outer radius $r_o$ and adjust the value of $r_t$ in (31) until the boundary conditions are met; this may make more sense since $r_t$ is somewhat arbitrary in the first place and might be related, on physical grounds, to the radius of maximum wind.

Before discussing numerical solutions of (31) and (35) with the imposed boundary conditions, it is helpful to derive analytic solutions valid in the region for which $V >> fr$. In this case, it is easily shown that one can neglect the second term in the square root appearing in (35) as well as the first term on the right side of (32). Then (31) and (35) can be directly integrated and the boundary conditions

$$V = 0 \quad at \quad r = r_o$$

and

$$T = T_o \quad at \quad r = r_m$$

applied, where $r_m$ is the radius of maximum winds. The resulting expression for $V$ can be maximized with respect to $r$ to find the radius of maximum gradient winds and the maximum gradient wind. The outer radius, $r_o$, can also be found. Among the parameters $r_t$, $r_m$, and $r_o$, only one may be regarded as a free parameter; once one is specified, the other two are determined. We choose to regard $r_o$ as the free parameter of the problem, given that it is more or less and randomly distributed in nature (Chavas and Emanuel, 2010).

The asymptotically valid solution is most easily written in terms of angular momentum:

$$\left(\frac{M}{M_m}\right)^{2-\frac{C_k}{C_D}} = \frac{2\left(\frac{r}{r_m}\right)^2}{2-\frac{C_k}{C_D}+\frac{C_k}{C_D}\left(\frac{r}{r_m}\right)^2}, \tag{36}$$

where $M_m$ is the angular momentum at the radius of maximum winds, whose relationship to $r_o$ may be found from (36) by requiring that $M = \frac{1}{2} fr_o^2$ at the outer radius:

$$\left(\frac{fr_o^2}{2V_m r_m}\right)^{2-\frac{C_k}{C_D}} = \frac{2\left(\frac{r_o}{r_m}\right)^2}{2-\frac{C_k}{C_D}+\frac{C_k}{C_D}\left(\frac{r_o}{r_m}\right)^2}. \tag{37}$$

For a reasonably intense vortex for which $V_m >> fr_m$ (which must be satisfied in any case for this asymptotic solution to be valid), and for which $r_o >> r_m$, (37) reduces approximately to

$$r_m \cong \frac{1}{2} fr_o^2 V_m^{-1}\left(\frac{1}{2}\frac{C_k}{C_D}\right)^{\frac{1}{2-\frac{C_k}{C_D}}}. \tag{38}$$

The maximum wind speed, $V_m$, found from maximizing the radial dependence of wind speed in the solution (36) is given by

$$V_m^{2-\frac{C_k}{C_D}} = V_p^2 \left( \frac{2r_m}{fr_o^2} \right)^{\frac{C_k}{C_D}}, \tag{39}$$

where $V_p$ is a velocity scale derivable strictly from environmental parameters:

$$V_p^2 \equiv \frac{C_k}{C_D} \left( T_b - T_o \right) \left( s_0 * - s_e * \right). \tag{40}$$

Substituting (38) into (39) gives

$$V_m^2 \cong V_p^2 \left( \frac{1}{2} \frac{C_k}{C_D} \right)^{\frac{\frac{C_k}{C_D}}{2-\frac{C_k}{C_D}}}. \tag{41}$$

Using this and (40) in (38) gives

$$r_m \cong \left( \frac{1}{2} \right)^{\frac{3}{2}} \frac{fr_o^2}{\sqrt{\left( T_b - T_o \right) \left( s_0 * - s_e * \right)}}. \tag{42}$$

Remarkably, the relationship between the radius of maximum winds and the outer radius does not depend on the exchange coefficients, to the extent that the applied approximations are valid.

One final relationship that comes from application of the boundary conditions is

$$r_t^2 = r_m^2 \frac{C_D}{C_k} Ri_c. \tag{43}$$

This completes the specification of the asymptotic solution valid where $V >> fr$. There are several noteworthy aspects of this solution. First, the factor multiplying the nominal potential intensity in (41) somewhat reduces the sensitivity of the overall solution to the ratio $C_k / C_D$. While at first glance it appears that (41) contains a singularity, it is in fact continuous through $C_k = 2C_D$. Figure 8 compares the dependence of the maximum wind speed on this ratio to the square root dependence that would be inferred from a naïve application of (22). As noted by Bryan and Rotunno (2009) and others, the dependence of numerically simulated peak hurricane winds on the ratio of exchange coefficients is weaker than the square root dependence in regimes for which the actual wind is approximately equal to the gradient wind (though they noted that this dependence is also a function of the turbulent mixing lengths). This can be understood by close examination of (22). As the drag coefficient increases, the multiplicative factor in front of the right side decreases, but so too does the boundary layer enthalpy, $k$,

because of increased inflow. This second effect tends to increase the surface enthalpy flux, partially offsetting the increased dissipation associated with increased drag coefficient. Also note that when $C_k = C_D$, (41) shows that the potential intensity is reduced from the value given by (40) by the square root of ½. And, in the limit $C_D \to 0$, the potential intensity approaches $\sqrt{2}$ time the nominal value given by (40) evaluated with $C_k = C_D$.

The radius of maximum winds given by (42) increases with the square of the outer radius, and linearly with the Coriolis parameter. It becomes smaller with increasing (nominal) potential intensity.

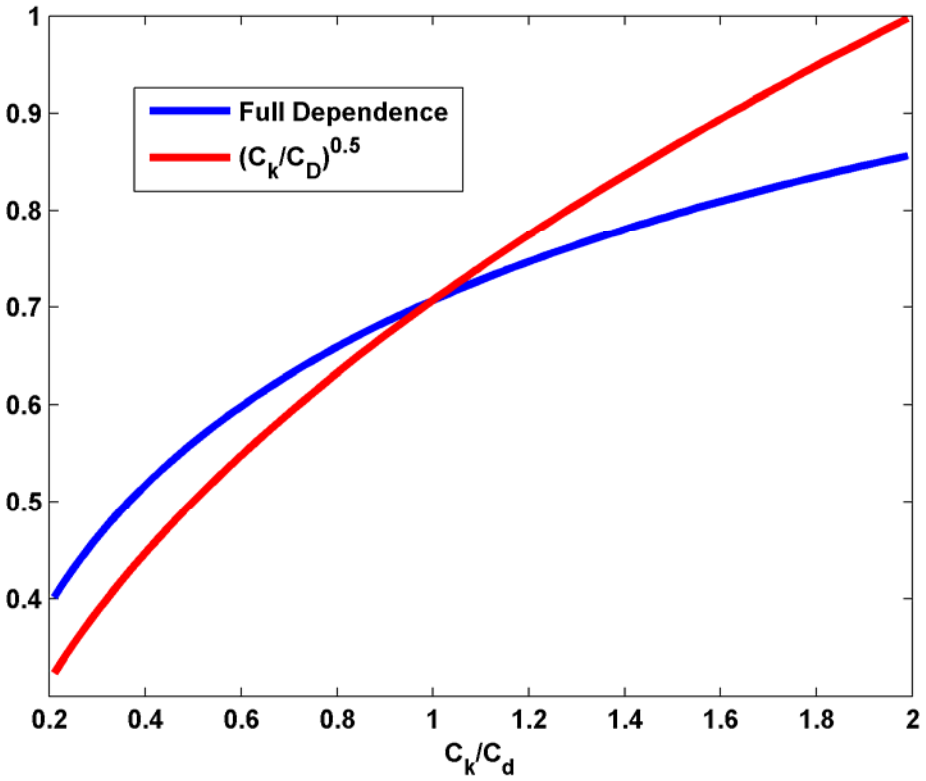


**Figure 8: Dependence of wind speed on the ratio of exchange coefficients inferred from (41) (blue) compared to a square-root dependence (red).**

Figure 9 compares the aforementioned analytic approximate solution to a numerical solution of (31) and (35). The analytic solution is such a good approximation to the numerical solution of the full equations through the whole range of radii that one might suspect that it is an exact solution. Experiments varying the ratio of exchange coefficients indeed show that the two solutions are almost identical through a wide range of conditions, but if the potential intensity is made small enough, differences begin to appear. For hurricane strength vortices, the analytic solution given by (36), (41), and (42) is an excellent approximation to the full solution.

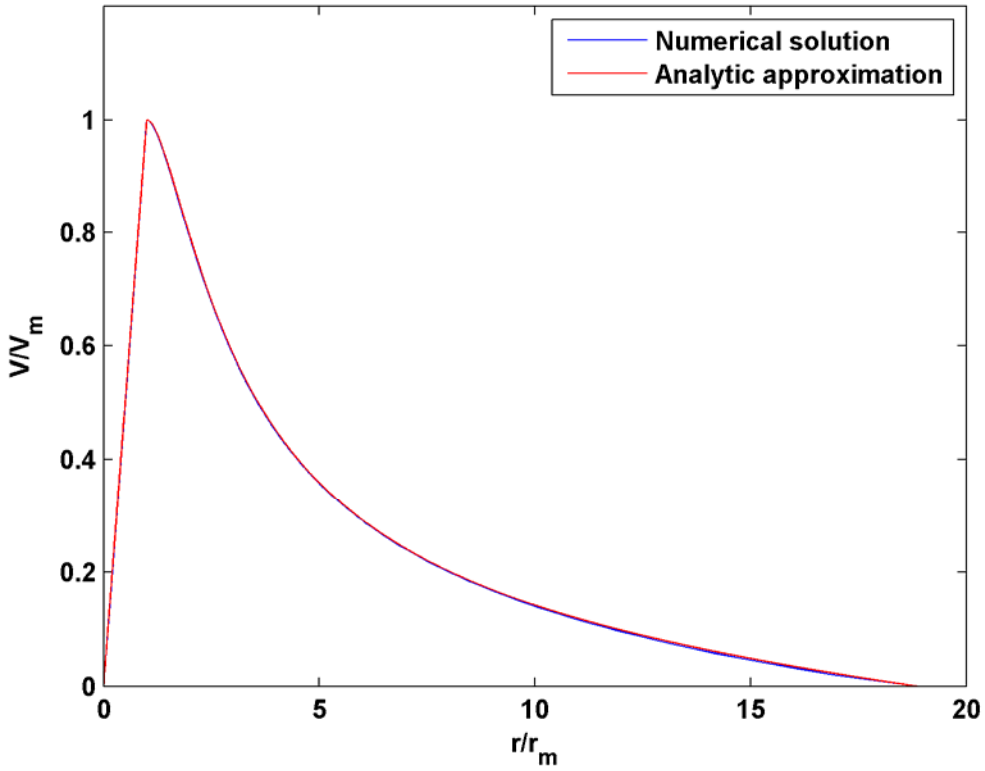


**Figure 9: Numerical solution of (31) and (35) (blue) compared to the analytic solution (red) described in the text. Gradient wind has been normalized by its peak value, and radius has been normalized by the radius of maximum winds.**

Figure 10 compares full steady-state solutions for the radial profile of gradient wind in the steady state model to radial profiles of azimuthal wind 12 grid points (3.75 km) above the surface, averaged over the last 24 hours of the numerical integration of the RE87 model described in the previous section. The comparison is carried out for three different values of the ratio of the surface exchange coefficients of enthalpy and momentum. The theory and model solutions agree well, except in the outer region where the vertical motion is downward into the boundary layer; in such regions there is little reason to expect that the critical Richardson number argument applies. What determines the radial structure of hurricanes in the downflow region? One argument, presented by Emanuel (2004), is that the Ekman suction velocity corresponding to the radial profile of gradient wind must match the subsidence velocity that balances clear-sky radiative cooling in the regions devoid of deep convection. Also note in Figure 10 that the match between the theoretical and model solutions is not so good when $C_k / C_D = 1.5$, but the predicted peak winds match the model results quite well in all three cases.

Some aspects of the dependence of tropical cyclones on the ratio of exchange coefficients that emerge from the steady-state model can be easily tested in the full RE87 numerical simulation. Figure 11a shows the evolution of the domain peak wind speed with time in five simulations that differ only in

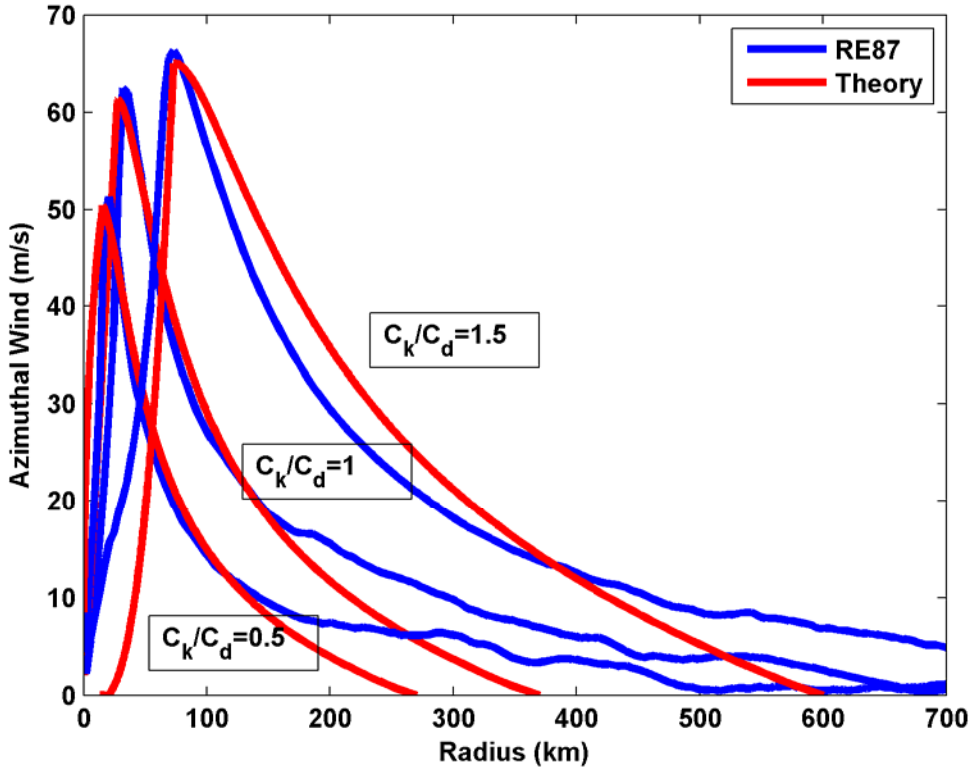


**Figure 10: Solutions of the steady-state model described in the text (red) compared to the radial profiles of azimuthal wind 12 grid points above the surface, averaged over the last 24 hours of three simulations using the RE87 model (blue). The three pairs of curves correspond to three different ratios of the surface exchange coefficients, as given by the values in the boxes. The outer radius of the steady-state model has been chosen in each case to yield a good match between the predicted and modeled radii of maximum winds.**

the ratio of the exchange coefficients. The simulations with higher values of the ratio develop more quickly and to higher intensities. Figure 11b shows the same fields but with the wind speeds normalized by

$$\left(2^{1-\frac{C_k}{C_D}}\frac{C_k}{C_D}\right)^{\frac{1}{2-\frac{C_k}{C_D}}} \tag{44}$$

according to (40) and (41), and time normalized by $\sqrt{\frac{1}{C_k}}$ (for reasons to be described in Part II). Bear in mind that while the simulations begin with the same actual intensity, their normalized initial intensities differ. Even with this caveat, the scaled intensity evolutions collapse nearly into a common evolution. This suggests that the steady-state model successfully predicts the dependence of the steady-state gradient wind on the ratio of exchange coefficients.

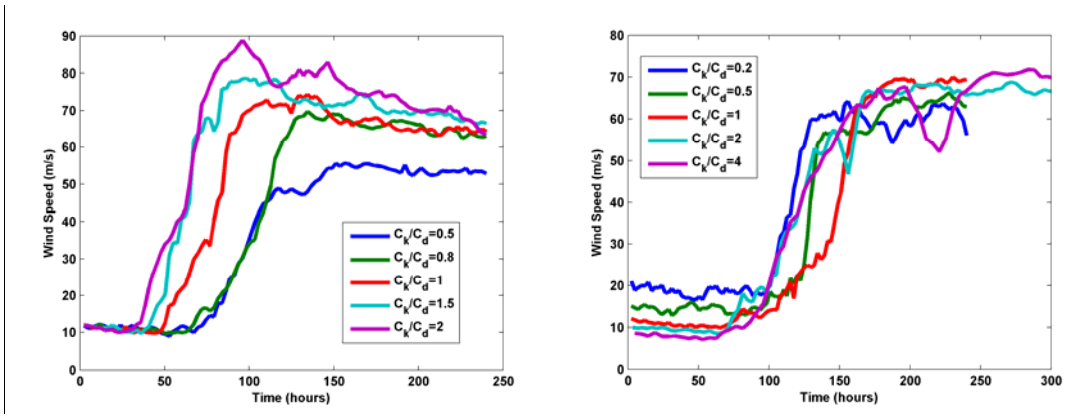


**Figure 11: Evolution with time of the peak surface wind in simulations of varying surface enthalpy exchange coefficient. In the graph on the right, the wind speeds have been normalized using (44) and time has been normalized by the inverse square-root of the enthalpy exchange coefficient.**

## 5. Summary

Analytic models of idealized, steady-state, axisymmetric tropical cyclones have assumed that the outflow streamlines asymptotically approach altitudes at which their entropy values match those of the undisturbed environment. We here showed that this is not the case in numerically simulated tropical cyclones, in which the outflow entropy stratification appears to be a product of the internal storm dynamics. We postulate that the entropy stratification is determined by a requirement that the Richardson Number not fall below a critical value, and analysis of numerically simulated storms suggests that this hypothesis has merit. A new steady-state model was developed based on this hypothesis and shown to produce physically realistic results; asymptotic solutions to this model are available for the case in which dissipative heating is neglected. As was true in all previous analytic models of this kind, a single radial length scale must be externally specified, but given this specification, the radial geometry of the storm is determined by the model. Given an outer radius, $r_o$, at which the storm's gradient wind is taken to vanish, the radial profile of the gradient wind is given to a good approximation by (42), (41), and (36). The revised model exhibits a weaker dependence on the ratio of exchange coefficients than the square-root dependence cited in earlier literature, but consistent with the results of numerical simulations using full-physics models. The increase in outflow temperature with radius outside the storm's core dictates the fall-off of gradient wind with radius; this radial profile of gradient wind is in good agreement with that produce by full-physics models. In Part II we shall examine the consequences of outflow self-stratification for the intensification of tropical cyclones.

## References

Bister, M., and K. A. Emanuel, 1998: Dissipative heating and hurricane intensity. *Meteor. Atmos. Physics*, **50,** 233-240,

——, 2002: Low frequency variability of tropical cyclone potential intensity, 1: Interannual to interdecadel variability. *J. Geophys. Res.*, **107,** doi:10.1029/2001JD000776,

Bryan, G. H., and R. Rotunno, 2009a: Evaluation of an analytical model for the maximum intensity of tropical cyclones. *J. Atmos. Sci.*, **66,** 3042-3060, doi:10.1175/2009JAS3038.1.

——, 2009b: The maximum intensity of tropical cyclones in axisymmetric numerical model simulations. *Mon. Wea. Rev.*, **137,** 1770-1789, doi:10.1175/2008MWR2709.1.

Chavas, D. R., and K. A. Emanuel, 2010: A QuickSCAT climatology of tropical cyclone size. *Geophys. Res. Lett.*, **37**, 10.1029/2010GL044558.

Emanuel, K., 2004: Tropical cyclone energetics and structure. *Atmospheric Turbulence and Mesoscale Meteorology*, R. R. a. B. S. E. Federovich, Ed., Cambridge University Press, 240.

Emanuel, K. A., 1983: On assessing local conditional symmetric instability from atmospheric soundings. *Mon. Wea. Rev.*, **111,** 2016-2033.,

——, 1986: An air-sea interaction theory for tropical cyclones. Part I. *J. Atmos. Sci.*, **42,** 1062-1071,

——, 1997: Some aspects of hurricane inner-core dynamics and energetics. *J. Atmos. Sci.*, **54,** 1014-1026,

Kepert, J. D., 2010: Slab- and height-resolving models of the tropical cyclone boundary layer. Part I: Comparing the simulations. *Quart. J. Roy. Meteor. Soc.*, **134,** in press,

Kleinschmidt, E., Jr., 1951: Gundlagen einer Theorie des tropischen Zyklonen. *Archiv fur Meteorologie, Geophysik und Bioklimatologie, Serie A*, **4,** 53-72,

Rotunno, R., and K. A. Emanuel, 1987: An air-sea interaction theory for tropical cyclones. Part II. *J. Atmos. Sci.*, **44,** 542-561,

Shutts, G. J., 1981: Hurricane structure and the zero potential vorticity approximation. *Mon. Wea. Rev.*, **109,** 324-329,

Smith, R. K., M. T. Montgomery, and S. Vogl, 2008: A critique of Emanuel's hurricane model and potential intensity theory. *Quart. J. Roy. Meteor. Soc.*, **134,** 551-561,